

1 Article

2 Performance of Resource Allocation in 3 Device-to-Device Communication Systems Based on 4 Evolutionally Optimization Algorithms

5 Tan-Hsu Tan¹, Bor-An Chen¹ and Yung-Fa Huang^{2,*}

6 ¹ National Taipei University of Technology; thtan@ntut.edu.tw

7 ² Chaoyang University of Technology; yfahuang@cyut.edu.tw

8 * Correspondence: yfahuang@cyut.edu.tw; Tel.: +886-4-2332-3000

9

10 **Abstract:** In this study, the resource blocks (RB) are allocated to user equipment (UE) according to
11 the evolutionary algorithms for long term evolution (LTE) systems. Particle Swarm Optimization
12 (PSO) algorithm is one of the evolutionary algorithms, based on the imitation of a flock of birds
13 foraging behavior through learning and grouping the best experience. In previous work, the
14 Simple Particle Swarm Optimization (SPSO) algorithm was proposed for RB allocation to enhance
15 the throughput of Device-to-Device (D2D) communications and improve the system capacity
16 performance. In simulation results, with less population size of $M=10$, the SPSO can perform
17 quickly convergence to sub-optimal solution in the 100th generation and obtained sub-optimum
18 performance with more 2 UEs than the Rand method. Genetic algorithm (GA) is one of the
19 evolutionary algorithms, based on Darwinian models of natural selection and evolution. Therefore,
20 we further proposed a Refined PSO (RPSO) and a novel GA to enhance the throughput of UEs and
21 to improve the system capacity performance. Simulation results show that the proposed GA with
22 100 populations, in 200 generations can converge to suboptimal solutions. Therefore, with
23 comparing with the SPSO algorithm the proposed GA and RPSO can improve system capacity
24 performance with 1.8 and 0.4 UEs, respectively.

25 **Keywords:** device-to-device; LTE systems; resource allocation; particle swarm optimization
26 algorithm; genetic algorithm; system capacity

27

28 1. Introduction

29 Orthogonal frequency division multiple access (OFDMA) combines the orthogonal frequency
30 division multiplexing (OFDM) and frequency division multiple access (FDMA) technology, for
31 multiple access of multiple users with high data rate. The OFDMA scheme in the fourth generation
32 mobile communication system (4G) long term evolution (LTE) technology not only upgrades
33 spectrum efficiency but also provides high resistance for frequency-selective fading channels [1].
34 The Device-to-Device (D2D) is a developing key technique for next generation (5G) mobile
35 communication systems [2]. The D2D technique allows unauthorized users equipments (UEs) to
36 access unused authorized cellular UE band, thereby improving the utilization efficiency of
37 bandwidth resource.

38 The D2D can maximize communications services in adjacent areas due to transfer data without
39 going through the base station. For example, the regional transmission and Wi-Fi combined [3,4]
40 can provide more neighboring users multimedia services, or find a nearby friend, real-time
41 communications conversations, and product advertising. It also has the potential to be applied in
42 settings of emergency medicine [5] and disaster scene [6] where patients far outnumber healthcare
43 providers and the outreaching communication bandwidth is limited.

44 In this study, the resource blocks (RBs) are allocated to UEs according to the evolutionary
 45 algorithms for LTE systems. The advantages of D2D techniques are such as improving energy
 46 efficiency of transmission, energy saving [7] and coverage rate improvement [6]. In the serious
 47 interfering environments of communication systems, most of directly transmission UEs cannot
 48 reach transmission rate requirement when the UEs is far from the base station. However, with relay
 49 station for transmission, most UEs can reach the minimum requirements of transmission rate [10].
 50 Therefore, the application of relay station for transmission in the serious interference environment,
 51 the performance of system outperforms the directly transmission systems.

52 Particle Swarm Optimization (PSO) algorithm [8] is one of the evolutionary algorithms, based
 53 on the imitation of a flock of birds foraging behavior through learning and grouping the best
 54 experience. In previous works [8], a Simple Particle Swarm Optimization (SPSO) algorithm was
 55 developed for resources allocation to achieve quality of service (QoS) and to maximize system
 56 capacity. Therefore, in this paper, we further proposed a Refined PSO (RPSO) to enhance the
 57 throughput of UEs and to improve the system capacity performance

58 The GA is a stochastic search algorithm whose procedures are based on the Darwinian models
 59 of natural selection and evolution [9]. Given some arbitrary initial solutions, the GA will generate the
 60 better solution through a series of genetic operations including selection, crossover, and mutation.
 61 Furthermore, The GA searches the solution space in parallel, that is, a set of possible solutions are
 62 manipulated in the same generation, so multiple local optimum can be reached simultaneously and
 63 thereby the likelihood of finding the global optimum is increased. In previous works [10], we
 64 proposed a novel redundancy-saving genetic algorithm (RSGA) based on the cost value of the
 65 fitness function to improve the complexity in term the BER requirement for DS-CDMA systems.
 66 However, it is not suitable for OFDMA systems. Therefore, in this study, we further proposed a
 67 novel GA for the RB allocation for D2D systems.

68 2. System Models

69 In this paper the LTE communication systems based resources allocation issues are
 70 investigated. The systems architecture is shown in Fig. 1. In this hybrid system, D2D UEs and
 71 traditional Cellular users' equipments (CeUEs) share all resources. In Figure 1, totally three relay
 72 stations are deployed in the cellular system, where UEs are uniformly random distributed in relay
 73 stations. In this study, base station is located in the center, and three relay stations form a triangle
 74 around the base station. Each relay station signal coverage with radius of 200 m. The CeUEs are
 75 uniformly random distributed in each relay stations within range. Each D2D pair includes a
 76 receiver UE and a transmitter UE distributed with 80 m distance from relay station. Channel
 77 models include Raleigh Fading, Shadowing Fading and path loss [11].

78 In Figure 1, each uplink data transfer includes two hops. In the first hop, the u_i -th UE transmits
 79 signal to the l th relay station by channel gain $h_{u_i,l}^{(n)}$. The l th relay station relays the transmission to
 80 base station using the n th resource block (RB). However, when the u_j -th D2D UE transmits signal to
 81 the l th relay station, it will occurs the interference link gain $g_{u_j,l}^{(n)}$ to the l th relay station.

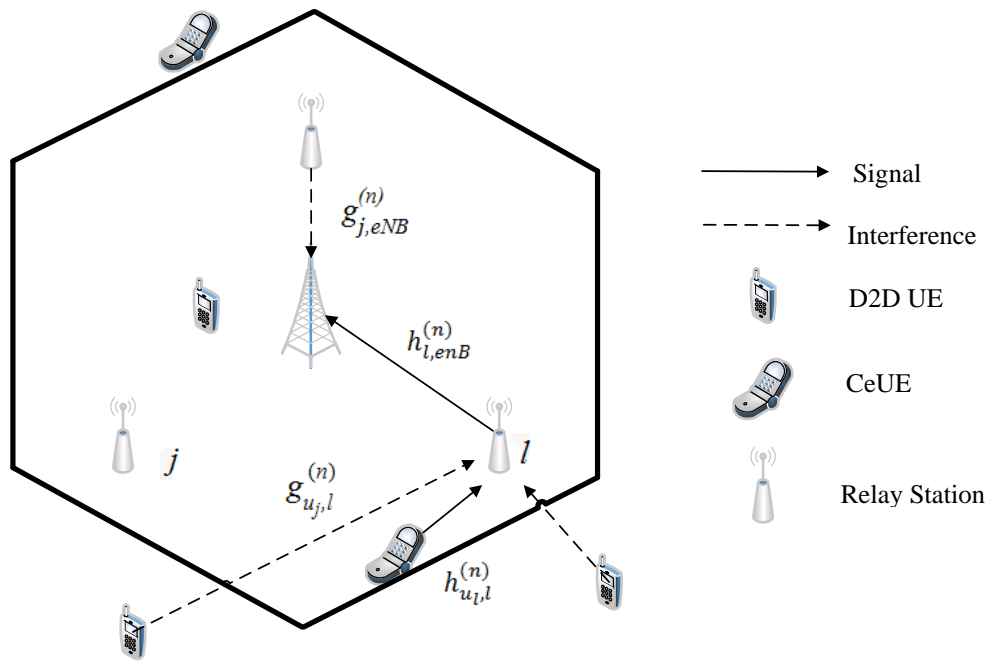
82 In this study, the channel models include path loss and shadowing fading. Thus, the fading
 83 channel model from UE to relay station (UE-relay) can be expressed by

$$84 \quad PL_{u_i,l}(\ell)_{[dB]} = 103.8 + 20.9 \log(\ell) + L_{su} + 10 \log(\zeta) \quad (1)$$

85 where 103.8 is antenna gain; L_{su} is shadowing fading with log-normal distributed random variable
 86 where the standard deviation $\sigma = 10$; $10 \log(\zeta)$ is Rayleigh fading effect, ℓ is the distance
 87 between UE to relay station. Similarly, the fading channel model from relay station to BS (relay-BS)
 88 can be expressed by [11]

$$89 \quad PL_{l,eNB}(\ell)_{[dB]} = 100.7 + 23.5 \log(\ell) + L_{su} + 10 \log(\zeta) \quad (2)$$

90



91

92

Figure 1. Systems architecture with deployment of three relay station.

93

94

It is assumed that Base Station (BS) has know well the Channel State Information (CSI) of all channels. Then, the unit Power Signal-to-Interference-Plus-Noise Ratio (Unit Power SINR) of the first hop can be expressed by

95

96

97

$$\gamma_{u_l,l,1}^{(n)} = \frac{P_{u_l,l}^{(n)} h_{u_l,l}^{(n)}}{\sum_{\substack{u_j \in U_j \\ j \neq l, j \in \mathcal{L}}} x_{u_j} P_{u_j,l}^{(n)} g_{u_j,l}^{(n)} + \sigma^2} \quad (3)$$

98

99

100

101

102

103

where $h_{u_l,l}^{(n)}$ is the channel gain from the u_l -th UE to the l -th relay with the n -th RB. $x_{u_l} = 1$ or 0. Each UE can only use one RB, $x_{u_l} = 1$ indicates with one RB, however, $x_{u_l} = 0$ indicates without any RB. U_j is the set of D2D UEs in the j -th relay area. $P_{u_l,l}^{(n)}$ and $P_{u_j,l}^{(n)}$ are transmission power of the u_l -th UE and the u_j -th CeUE, respectively. $g_{u_j,l}^{(n)}$ is the interference link gain from the u_j -th CeUE to the l -th relay. $\sigma^2 = N_0 B_{RB}$. N_0 is power spectral density of the added white Gaussian noise (AWGN). B_{RB} is bandwidth of an RB. Similarly, the unit power SINR of the second hop can be expressed by

104

$$\gamma_{l,eNB,2}^{(n)} = \frac{P_{l,eNB}^{(n)} h_{l,eNB}^{(n)}}{\sum_{\substack{u_j \in U_j \\ j \neq l, j \in \mathcal{L}}} x_{u_j} P_{j,eNB}^{(n)} g_{j,eNB}^{(n)} + \sigma^2} \quad (4)$$

105

106

107

108

109

110

where $h_{l,eNB}^{(n)}$ is the channel gain from the l -th relay to the Base Station (eNB) with the n -th RB. $P_{l,eNB}^{(n)}$ and $P_{j,eNB}^{(n)}$ are transmission power of the l -th relay and the j -th relay, respectively. $g_{j,eNB}^{(n)}$ is the interference link gain from the j -th relay to the eNB with the n -th RB.

In this study, there are two links in the second hop. Eq. (4) expresses the SINR of the l -th relay station to BS. Similarly, the SINR of the l -th relay station to the receiver of D2D pair can be expressed by

111

$$\gamma_{l,u_l,2}^{(n)} = \frac{P_{l,u_l}^{(n)} h_{l,u_l}^{(n)}}{\sum_{\substack{u_j \in U_j \\ j \neq l, j \in \mathcal{L}}} x_{u_j} P_{j,u_l}^{(n)} g_{j,u_l}^{(n)} + \sigma^2} \quad (5)$$

112

113

In Eqs. (3)-(5), the SINR for all the links will be obtained. Then the throughput (Kbps) of the first hop can be derived by

114

$$r_{u_l,1}^{(n)} = B_{RB} \log_2(1 + \gamma_{u_l,1}^{(n)}) \quad (6)$$

115

Similarly, the throughput of the second hop can be obtained by

$$116 \quad r_{u_l,2}^{(n)} = B_{\text{RB}} \log_2(1 + \gamma_{l,u_l}^{(n)}) \quad (7)$$

117 Thus, the throughput for the n th RB by the user u_l can be obtained by

$$118 \quad R_{u_l}^{(n)} = \frac{1}{2} \min\{r_{u_l,1}^{(n)}, r_{u_l,2}^{(n)}\} \quad (8)$$

119 With Eq. (8), the total throughput of N RBs is $\sum_{l \in L} \sum_{u_l \in U_l} \sum_{n=1}^N x_{u_l}^{(n)} R_{u_l}^{(n)}$. All UEs are desired to
 120 obtain the RBs to reach the maximal throughput. Therefore, to avoid deteriorating the
 121 communication quality a threshold Q_{u_l} is set to meet the required throughput for most UEs. Some
 122 constraints are set to perform the optimization problem as

$$\begin{cases} \sum_{u_l \in U_l} x_{u_l}^{(n)} \leq 1, \forall n \in N & (9a) \\ \sum_{n=1}^N x_{u_l}^{(n)} P_{u_l}^{(n)} \leq P_{u_l}^{\max}, \forall u_l \in U_l & (9b) \\ \sum_{n=1}^N x_l^{(n)} P_{l,u_l}^{(n)} \leq P_l^{\max}, \forall u_l \in U_l & (9c) \\ R_{u_l} \geq Q_{u_l}, \forall u_l \in U_l & (9d) \end{cases}$$

123

124 where Eq. (9a) set the constraints for that each UE use only one RB. Eq. (9b) and (9c) are the
 125 constraints on the minimum power for UEs and relay stations, respectively. Eq. (9d) is the
 126 minimum throughput requirements of QoS for UEs.

127 Moreover, the interference of the first hop and the second hop for system is expressed by

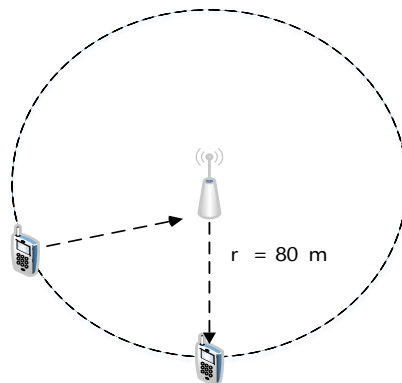
$$128 \quad I_{u_l,1}^{(n)} = \sum_{\substack{u_j \in U_j \\ j \neq l, j \in L}} x_{u_j}^{(n)} P_{u_j,l}^{(n)} g_{u_j,l}^{(n)} \quad (10)$$

129 and

$$130 \quad I_{u_l,2}^{(n)} = \begin{cases} \sum_{\substack{u_j \in U_j \\ j \neq l, j \in L}} x_{u_j}^{(n)} P_{j,eNB}^{(n)} g_{j,eNB}^{(n)}, u_l \in \{C \cap U_l\} \\ \sum_{\substack{u_j \in U_j \\ j \neq l, j \in L}} x_{u_j}^{(n)} P_{j,u_l}^{(n)} g_{j,u_l}^{(n)}, u_l \in \{D \cap U_l\} \end{cases} \quad (11)$$

131 , respectively.

132 In the system model, it is assumed that the base station coverage area is a circle with the radius
 133 175 m. In this area, there are three relay station uniformly deployed with a triangle as shown in
 134 Figure 1. The coverage area of each relay station is a circle with radius 100 m. The cellular UEs are
 135 uniformly random distributed around the relay station. D2D pairs are deployed on a circle with
 136 radius 80 m around each relay station as shown in Figure 2. The numbers of UEs in the relay station
 137 are the same. It is assumed that the CSI of the links are known to base station. The simulation
 138 parameters are listed in Table 1.



139

140

Figure 2. D2D pairs deployed on the circle around the relay station.

141

Table 1. System simulation parameters.

System bandwidth (MHz)	2.5
Bandwidth of subcarrier (Hz)	1500
Number of RBs	13
Radius of the coverage area of relay station (meter)	200
Distance between base station and relay station (meter)	125
Number of CeUE	9, 12, 15
Number of D2D pairs	3, 6, 9
Minimum distance between base station and UEs (meter)	10
Power of relay station (P_r , dBm)	30
Power of UEs (P_{u_i} , dBm)	23
Minimum throughput requirements of CeUEs ($R_{th,C}$, Kbps)	128
Minimum throughput requirements of D2D pairs ($R_{th,D}$, Kbps)	256
Standard deviation of Shadowing fading between relay and BS (dB)	6
Standard deviation of Shadowing fading between UEs and relay station (dB)	10
Power Spectral density of AWGN (dBm/Hz)	-174

142

143 3. PSO based Resource Allocation

144 PSO algorithms are used to simulate the bird swarm foraging situation, which is in the search
 145 for food space with particles. Each particle simulates a bird, in addition to its own normal
 146 movement, also refer to its own best moving experience. The personal best experience is denoted by
 147 s^{pbest} . Then the global experience is referred from the group's best moving experience with global
 148 best, denoted by s^{gbest} . According to the above kinds of data with an iterative evolution, the final
 149 convergence obtains the optimal solution.

150 In this study, the number of particles is M , and the value of the particle's target function is the
 151 pointer to the efficiency of the iteration. The particle with the highest target function value is the
 152 best solution. A simplified formula for particle swarm optimization, called SPSO, is proposed to
 153 improve the performance of the resource allocation for D2D communication systems. The SPSO
 154 algorithm performs the optimization of resource block allocation, and all the relay stations cover the
 155 UEs of the allocated RB as the particle s_i . The particle is uniformly distributed in the solution space.
 156 Total 13 RBs and 3 relay stations are available. The moving velocity of the first particle in the
 157 $(g+1)$ -generation is expressed by

$$158 \quad \mathbf{v}_i^{g+1} = c_1 \times rand() \times (\mathbf{s}^{pbest} - \mathbf{s}_i^g) + c_2 \times rand() \times (\mathbf{s}^{gbest} - \mathbf{s}_i^g) \quad (12)$$

159 where \mathbf{s}_i^g is the position vector of the i th particle in g -generation, $\mathbf{s}_i^g = [s_{i_1}^g, \dots, s_{i_l}^g, \dots, s_{i_3}^g]$, and $\mathbf{s}_{i_l}^g$ is
 160 the position of the i th particle of the l th relay station. The local optimal positions of all particles are
 161 denoted by $\mathbf{s}^{pbest} = [s^{pbest_1}, \dots, s^{pbest_1}, \dots, s^{pbest_3}]$, where s^{pbest_l} is the local optimal position of the l th
 162 relay station. \mathbf{s}^{gbest} is the global optimal positions of all particles in the nearest generation. both c_1
 163 and c_2 are the acceleration coefficients, called by individual factor and social factor, respectively.
 164 Generally, the factors are set by $c_1=2$ and $c_2=2$. The $rand()$ is the random function with uniformly
 165 distributed in $[0,1]$.

166 Moreover, the position updating at $(g+1)$ -generation can be expressed by

$$167 \quad \mathbf{s}_i^{g+1} = \mathbf{s}_i^g + \mathbf{v}_i^{g+1} \quad (13)$$

168 In SPSO, all the K UEs distributed in the coverage area of relay station are allocated RBs and
 169 composited as a particle \mathbf{s}_i with an array of $1 \times K$. The M particles are uniformly distributed in the
 170 solution space, and a total of 13 RBs are available to be allocated to the UEs in three relay stations.

171 In SPSO the object function is defined by

$$172 \quad f_C = \sum_{u_i=1}^K y_{u_i} \quad (14)$$

173 where $\sum_{u_i=1}^K y_{u_i}$ is the system capacity and y_{u_i} is defined by

$$174 \quad y_{u_i} = \begin{cases} 1, & \sum_{n=1}^N x_{u_i}^{(n)} R_{u_i}^{(n)} \geq R_{th} \\ 0, & \text{otherwise} \end{cases} \quad (15)$$

175 The procedure of SPSO algorithms applied in this study can be described by the following
 176 example with $K=18$ and $M=3$:

177 1) Initialization ($g=1$): Generate the positions of M particles, $\mathbf{s}_i^1, \mathbf{s}_i^1, i=1, \dots, M$ and velocity, $\mathbf{v}_i^1, i=1,$
 178 \dots, M . One example of the position of a particle $\mathbf{s}_i^1, \mathbf{s}_i^1$ can expressed by $\mathbf{s}_1^1 = [1 \ 1 \ 3 \ 4 \ 5 \ 6 \ | \ 2 \ 8$
 179 $3 \ 11 \ 11 \ 13 \ | \ 1 \ 6 \ 7 \ 8 \ 4 \ 9]$.

180 2) Calculate the objective function value of all particles according to Eq. (8) and find the \mathbf{s}^{spb} and
 181 \mathbf{s}^{gbest} for this generation. One example of \mathbf{s}^{spb} and \mathbf{s}^{gbest} can be $\mathbf{s}^{spb_1} = [1 \ 1 \ 3 \ 4 \ 5 \ 6]$; \mathbf{s}^{spb_2}
 182 $= [7 \ 8 \ 9 \ 10 \ 11 \ 12]$; $\mathbf{s}^{spb_3} = [1 \ 3 \ 4 \ 5 \ 7 \ 6]$ and $\mathbf{s}^{gbest} = [3 \ 4 \ 5 \ 6 \ 7 \ 5 \ | \ 7 \ 8 \ 9 \ 10 \ 11 \ 12 \ | \ 1 \ 3 \ 4 \ 5 \ 7 \ 6]$,
 183 respectively.

184 3) Let $g=g+1$. According to step (2), we calculate the speed and position of the next generation ($g+1$)
 185 particle, after one generation calculation. Then one example of the position can be $\mathbf{s}_1^1 = [2 \ 3 \ 1 \ 4$
 186 $5 \ 6 \ | \ 9 \ 7 \ 6 \ 11 \ 13 \ 10 \ | \ 1 \ 6 \ 7 \ 8 \ 4 \ 9]$.

187 If the number of generations $g < G$, return to step (2) to update the individual optimal solution
 188 and the population optimal solution. One example can be as: the previous \mathbf{s}^{spb_1} is unchanged
 189 by $\mathbf{s}^{spb_1} = [1 \ 1 \ 3 \ 4 \ 5 \ 6]$. But the other two individual optimal solutions is updated by $\mathbf{s}^{spb_2} = [9$
 190 $7 \ 6 \ 11 \ 13 \ 10]$ and $\mathbf{s}^{spb_3} = [2 \ 7 \ 8 \ 9 \ 3 \ 5]$, respectively. Moreover, the new \mathbf{s}^{gbest} is updated
 191 according the object function by $\mathbf{s}^{gbest} = [2 \ 3 \ 1 \ 4 \ 5 \ 6 \ | \ 9 \ 7 \ 6 \ 11 \ 13 \ 10 \ | \ 1 \ 6 \ 7 \ 8 \ 4 \ 9]$.

192 4) If the number of generation is $g = G$, the calculation is ended.

193 Then after $N(N \leq G)$ generations, one of the positions \mathbf{s}_i^1 is selected by $\mathbf{s}_1^1 = [8 \ 4 \ 5 \ 7 \ 3 \ 2 \ |$
 194 $7 \ 8 \ 9 \ 10 \ 11 \ 12 \ | \ 1 \ 5 \ 4 \ 9 \ 6 \ 7]$. The global optimal solution \mathbf{s}^{gbest} is obtained by $\mathbf{s}^{gbest} = [2 \ 3 \ 1 \ 4 \ 5 \ 6 \ | \ 9$
 195 $7 \ 6 \ 11 \ 13 \ 10 \ | \ 1 \ 6 \ 7 \ 8 \ 4 \ 9]$. Hence, in this PSO calculation, the solution is $\mathbf{s}^{gbest} = [2 \ 3 \ 1 \ 4 \ 5 \ 6 \ | \ 9 \ 7 \ 6 \ 11$
 196 $13 \ 10 \ | \ 1 \ 6 \ 7 \ 8 \ 4 \ 9]$.

197 To upgrade effectiveness of SPSO, this research according to system schema of relay station
 198 partition characteristics on SPSO for optimization, in (12), the learning factor with weight parameter
 199 cw_1 and cw_2 , to speedup optimization searching. This PSO is called Refined PSO (RPSO). Then, its
 200 next generation of evolution speed of particle \mathbf{s}_i^{g+1} can be obtained by

$$201 \quad \mathbf{v}_i^{g+1} = c_1 \cdot \mathbf{cw}_1 \cdot \text{rand}() \times (\mathbf{s}^{pbest} - \mathbf{s}_i^g) + c_2 \cdot \mathbf{cw}_2 \cdot \text{rand}() \times (\mathbf{s}^{gbest} - \mathbf{s}_i^g) \quad (16)$$

202 where \mathbf{cw}_1 and \mathbf{cw}_2 are $1 \times K$ vector, where K is the number of UE, both on behalf of weights for
 203 adjusting the searching efficiency of particles.

204 The modifying rule of \mathbf{cw}_1 is the followings:

205 1) $\mathbf{cw}_1(u_i) = 1$ for that the RB of the u_i -th UE in \mathbf{s}^{pbest_i} does not conflict with the RBs of other relay
 206 stations.

- 207 2) $\mathbf{cw}_1(u_i) = 0$ for that the RB of the u_i -th UE in \mathbf{s}^{pbest_i} conflicts with the RBs of other relay
 208 stations once.
- 209 3) $\mathbf{cw}_1(u_i) = 3$ for that the RB of the u_i -th UE in \mathbf{s}^{pbest_i} conflicts with the RBs of other relay stations
 210 once more.
- 211 The modifying rule of \mathbf{cw}_2 is the followings:
- 212 1) $\mathbf{cw}_2(u_i) = 1$ for that the RB of the u_i -th UE in \mathbf{s}^{gbest} does not conflict with the RBs of UEs of other
 213 relay stations. $\mathbf{cw}_2(u_i) = 1$ for $g > 10$.
- 214 2) $\mathbf{cw}_2(u_i) = 3$ for that the RB of the u_i -th UE in \mathbf{s}^{gbest} conflicts with the RBs of other relay stations
 215 once or more in $g \leq 10$.

216 4. RB Allocation with GA Discussion

217 In genetic algorithms (GAs) [12,13], the main idea is to follow the fittest evolutionary laws of
 218 nature, by the procedures of selection, crossover and mutation to improve the fitness value of
 219 chromosomes. With GA, there are random search, and other ways to search for the optimal solution.
 220 Therefore, the GA is often used to apply on optimization issues. In this study, the GA is applied for
 221 resources allocation optimization, with the objective functions on maximal system capacity and
 222 throughput.

223 The procedures in GA are the followings: (1) data coding, (2) producing initial population, (3)
 224 calculation fitness values, (4) selection, (5) crossover, and (6) mutation. The procedures are
 225 proceeded iterated from (3) to (6), until meeting the terminated conditions. Then the solution are
 226 obtained as the optimal results.

227 In the parent group, it is in accordance with the fitness value of chromosomes, to determine
 228 whether it will be retained or eliminated. In the select operation in this study, the ranking method,
 229 ranks the fitness value of each chromosome. This method can avoid inbreeding [10].

230 The crossover of GA is by selecting two chromosomes from the mating pool, and swapping the
 231 genes into two new chromosomes. It is expected that crossover procedures can generate better
 232 offspring chromosomes. Higher crossover rate in GA will bring the higher evolutionary rate for the
 233 chromosomes.

234 The mutation can increase the ethnic diversity of GA operations. The aforementioned selection,
 235 crossover and other procedures in both groups search for better children, but its genetic
 236 characteristics must be associated with the parent. Because there are no new chromosomes joining
 237 the group in each generation, it makes that the searching area cannot be expanded. It will lead the
 238 evolution to converge earlier. However, through mutation, some new chromosomes will join the
 239 search space to avoid GA early convergence problems.

240 In GA the object function is defined by

$$241 \quad f_c = \sum_{u_i=1}^K y_{u_i} \quad (17)$$

242 where $\sum_{u_i=1}^K y_{u_i}$ is the system capacity and y_{u_i} is defined by

$$243 \quad y_{u_i} = \begin{cases} 1, & \sum_{n=1}^N x_{u_i}^{(n)} R_{u_i}^{(n)} \geq R_{th} \\ 0, & \text{otherwise} \end{cases} \quad (18)$$

244 5. Simulation Results

245 5.1. PSO

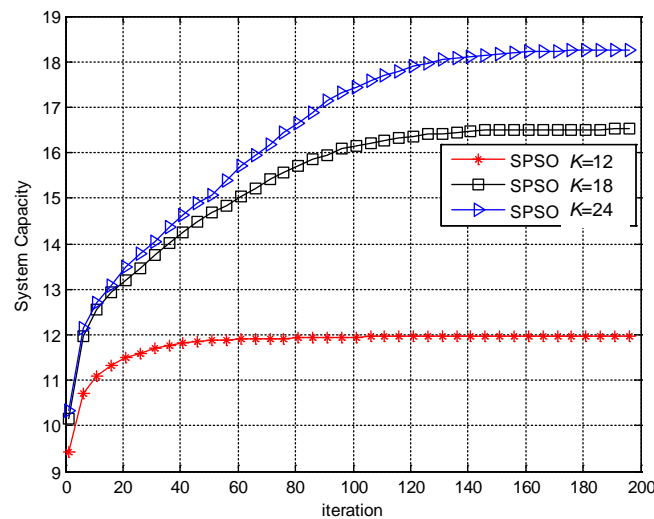
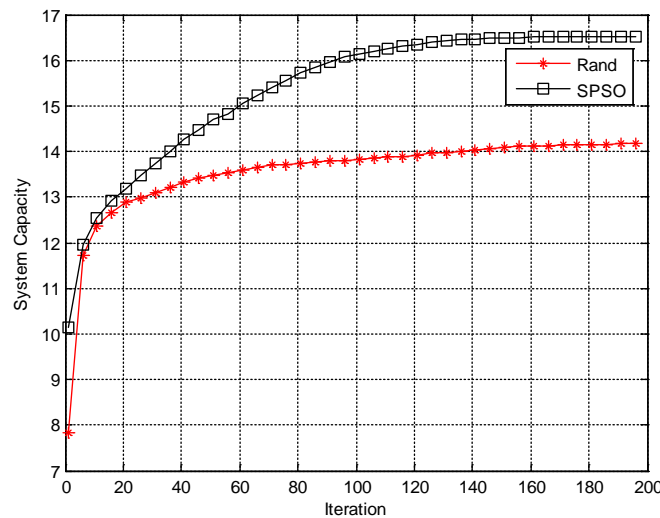
246 The simulation parameters based on SPSO and RPSO are shown in Table 2. In Figure 3,
 247 simulation results show that when the total number of UEs are $K = 12$, system capacity reaches 12
 248 UEs. However, when $K = 18$, the system capacity reaches 16.5 UEs. Moreover, when $K = 24$, system
 249 capacity is 18.3 UEs.

250 Figure 4 shows the comparisons between the proposed SPSO with $c_1=c_2=2$, $M=10$ and
 251 random allocation methods. The random method (Rand) is performed by random allocated the RBs
 252 to the UEs in each generation. But the system retains the best results to the next generation based on
 253 the same object function as SPSO. From Figure 4, it is easy to observe that the proposed SPSO
 254 outperform the Rand at the 20th iterations and highly improve the system capacity to 16 UEs at the
 255 100th iterations, which is 2 UEs more than that of Rand.

256

Table 2. Simulation parameters of PSO.

Maximal generations (G)	200
Number of particles (M)	10
Learning factors ($c_1=c_2$)	2
Number of user equipment (K) (Including CeUE and D2D UEs)	12, 18, 24
Number of relay station	3
ID of RBs	1 – 13

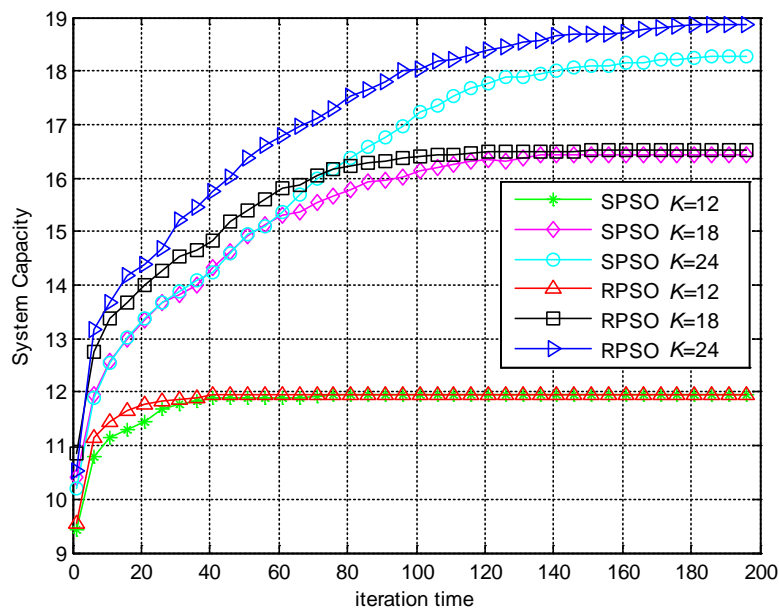
257
258**Figure 3.** Simulation results of SPSO method with $M=10$.

259

Figure 4. Simulation results comparisons between SPSO and random allocation method with $M=10$, $K=18$.

261 Figure 5 displayed the comparisons between RPSO and SPSO. In Figure 5, it is shown that
 262 RPSO speed up more than SPSO algorithm to converge the optimal for $K = 12$. Moreover, for $K = 18$
 263 and $K = 24$, system capacity of RPSO outperforms SPSO.

264 Table 3 shows the performance comparisons of SPSO, RPSO and random allocation (Rand) for
 265 $K=12, 18, 24$, with $M=10$, and $c_1=c_2 = 2$. Compared with the Rand, SPSO algorithm can improve the
 266 efficiency of about 17-20%, for $K=18, 24$. Moreover, the proposed RPSO algorithm can improve the
 267 efficiency of 18-24% than Rand.



268

269

Figure 5. The comparisons of convergence between RPSO and SPSO.

270

Table 3. The comparisons between RPSO, SPSO and Rand.

271

Number of UE (K)	12	18	24
a. RPSO	12	16.66	18.89
b. SPSO	12	16.52	18.3
c. Rand	11.8	14.1	15.2
$Gain_1$ ($a-c$)/ c	1.69%	18.16%	24.28%
$Gain_2$ ($b-c$)/ c	1.69%	17.16%	20.39%

272

273 5.2. GA

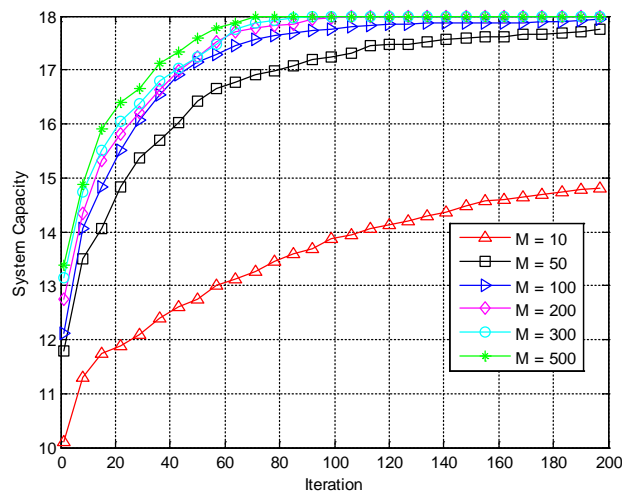
274 The simulation parameters based on GA are shown in Table 4. Figure 6 shows that the system
 275 capacity for different population size in GA with $K = 18$. The objective function is f_{obj_C0} in Eq.
 276 (12). When $M = 10$, the system capacity performance can reach 15 UEs. However, when $M \geq 100$,
 277 the system capacity reaches saturated with near optimal solution with 18 UEs. From Figure 6, it is
 278 observed that the large population size can reach the optimal solution.

279 Table 5 shows the performance comparisons of RPSO, GA and Rand methods with $M=100$ and
 280 $G=200$. From the results in Table 5, it is observed that the when $M=100$, the proposed GA
 281 outperform RPSO with 1.4 UEs of system capacity for $K=24$.

282

Table 4. Simulation parameters in GA.

Maximal generations (G)	200
Number of chromosomes (M)	10-500
Crossover rate (R_c)	0.9
Mutation rate (R_m)	0.07



283

284

Figure 6. System capacity for various population size with $K = 18$.

285

Table 5. System capacity comparisons of RPSO, GA and Rand methods with $M=100$ and $G=200$.

K	12	18	24
GA	12	17.96	21.8
RPSO	12	17.86	20.41
Rand	12	15.08	16.27

286

287 5.3. QoS Based Capacity Maximization

288 In this section, the Quality of Service (QoS) based system capacity maximization are
 289 investigated. The QoS based multi-object function can be written as

$$290 f_{\alpha} = \alpha \cdot f_C + (1 - \alpha) f_R \quad (19)$$

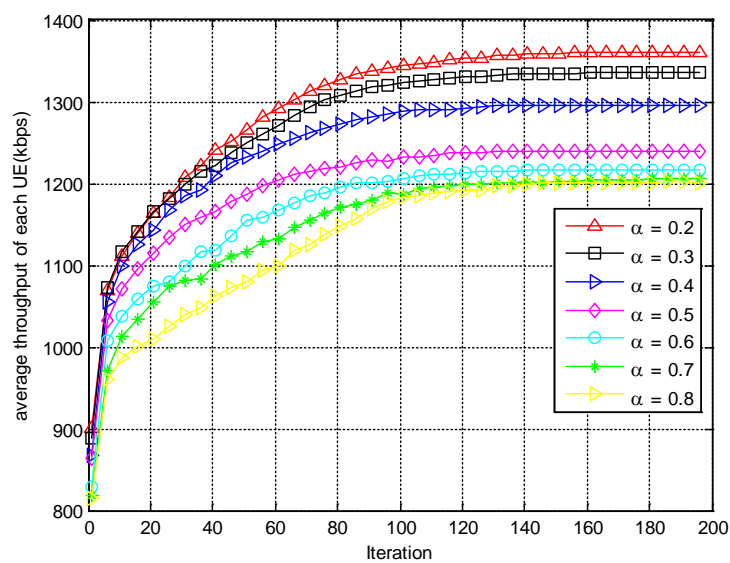
291 where α is the weighting factor for balance between capacity and throughput and the object
 292 function for system throughput is defined by

293

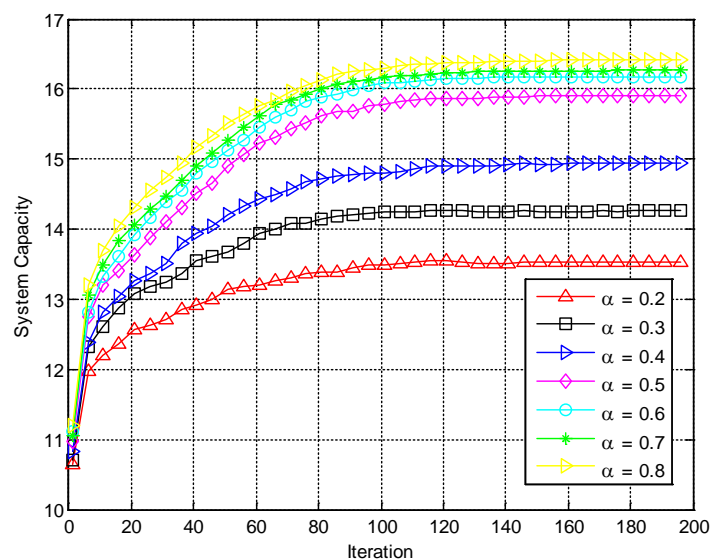
$$f_R = \sum_{n=1}^N x_{u_i}^{(n)} R_{u_i}^{(n)} \quad (20)$$

294 where $x_{u_i}=1$ or 0. Each UE can only use one RB, $x_{u_i}=1$ indicates with one RB. And $R_{u_i}^{(n)}$ is the
 295 throughput for the n th RB used by the user u_i .

296 Figure 7 shows the simulated results with different weight values for $UE=18$, which
 297 respectively represent the transmission capacity and system capacity of each UE. In Figure 7(a),
 298 during the period of about the first 10 generations of this period, regardless of the numerical value,
 299 the rate of increase of the average throughput is similar, indicating that the weight value has little
 300 effect. But after the number of generations exceeds 10 generations, the weighting starts to take
 301 effect. The smaller the weight value, the larger the amount of transmission. Figure 7(b) shows that
 302 after more than 10 generations, the larger the weight, the larger the system capacity. This result
 303 indicates that there is a conflict between maximizing the system capacity and the individual
 304 throughput of UEs.

305
306

(a)

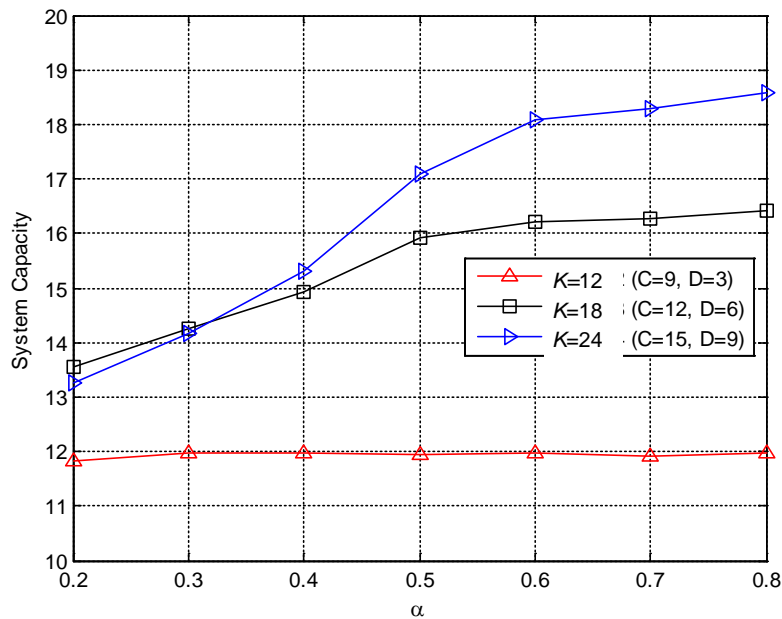
307
308

(b)

309 **Figure 7.** System performance comparisons in 200 generations for (a) throughput (b) system
 310 capacity with $K = 18$.

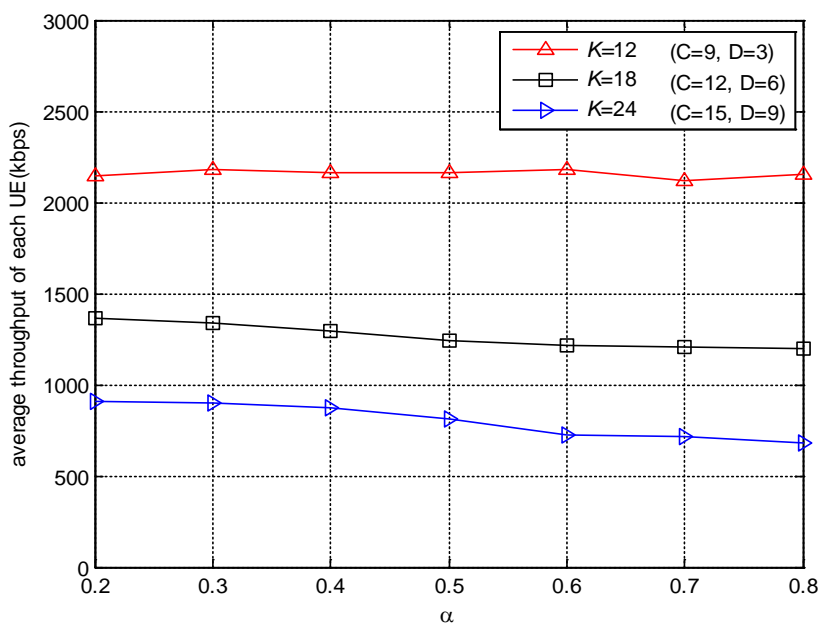
311 Figure 8 shows the comparison between the system capacity and the throughput obtained for $K = 12, 18,$
 312 24. In Figure 8(a), the more UEs are found, the greater the difference in performance, indicating that the
 313 transmission capacity and system capacity are increasing. After the complex situation is raised to a certain
 314 value, the mutual influence is greater, and the difference is the largest at 0.5-0.6.

315 In this study, the system capacity is taken as the higher priority requirement, and then the weighting is set
 316 to 0.6 according to Fig. 8. Under this weighting parameter, the system capacity when $K = 18$ can reach close to
 317 16 UEs. Moreover, Figure 8(b) shows the comparison of the throughput of each UE under the condition of
 318 $\alpha=0.2-0.8$. When $\alpha=0.6$ and $K = 18$, the throughput can still reach 1300 Kbps, and the system capacity can
 319 reach 16 UEs. Therefore, with the proposed multi-objective function, not only the throughput can be approved
 320 transmission, but also system capacity can be guaranteed.



321
 322

(a)



323

324

(b)

325

Figure 8. The comparisons of (a) system capacity and (b) throughput for different weighting α .

326 **6. Conclusions**

327 In this paper, the PSO algorithm is proposed to optimize resource allocation in D2D system.
328 Simulation results show that resource allocation optimization is performed using proposed RPSO
329 can significantly improve the system capacity performance. In this paper, the GA is proposed to
330 optimize resource allocation in D2D systems. Simulation results show that the proposed GA can
331 improve the system capacity performance. With population size $M=100$ and generations $g=200$, the
332 proposed GA can outperform the proposed SPSO 1.8 users for system capacity.

333 **Acknowledgments:** This work was funded in part by Ministry of Science and Technology of Taiwan under Grant MOST
334 106-2221-E-324-020.

335 **Author Contributions:** Tan-Hsu Tan and Yung-Fa Huang conceived and designed the experiments; Bor-An
336 Chen performed the experiments; Tan-Hsu Tan and Yung-Fa Huang analyzed the data; Tan-Hsu Tan
337 contributed analysis tools; Yung-Fa Huang wrote the paper.

338 **Conflicts of Interest:** The founding sponsors had no role in the design of the study; in the collection, analyses,
339 or interpretation of data; in the writing of the manuscript, and in the decision to publish the results.

340 **References**

- 341 1. Yun, L.; Le, Z.; Xin, T.; Bin, C. An advanced spectrum allocation algorithm for the across-cell D2D
342 communication in LTE network with higher throughput. *China Commun.* **2016**, *13*, 30-37.
- 343 2. Camps-Mur, D.; Garcia-Saavedra, A.; Serrano, P. Device-to-device communications with Wi-Fi direct:
344 overview and experimentation. *IEEE Wireless Commun.* **2013**, *20*, 96-104.
- 345 3. 3GPP- The Mobile Broadband Standard (Rel. 14). <http://www.3gpp.org/>(accessed on 30 March 2018).
- 346 4. Hara, S.; Prasad, R. *Multicarrier Techniques for 4G Mobile Communications*. Artech House Boston London,
347 2003.
- 348 5. Hasan, M.; Hossain, E. Resource Allocation for Network-Integrated Device-to-Device Communications
349 Using Smart Relays. In Proceedings of IEEE Globecom Workshops. Dec. 2013, 591–596,
- 350 6. Babun, L. Extended Coverage for Public Safety and Critical Communications Using Multi-hop and D2D
351 Communications," Master thesis, Department of Electrical Engineering, Florida International University,
352 Mar. 2015.
- 353 7. L. Wang, T. Peng, Y. Yang, and W. Wang, "Interference Constrained D2D Communication with Relay
354 Underlying Cellular Networks," In Proceedings of IEEE Vehicular Technology Conference, pp. 1-5, Sept.
355 2013.
- 356 8. Huang, Y.-F.; Tan, T.-H.; Chen, B.-A.; Liu, S.-H.; Chen, Y.-F. Performance of Resource Allocation in
357 Device-to-Device Communication Systems Based on Particle Swarm Optimization. In Proceedings of
358 2017 IEEE International Conference on Systems, Man, and Cybernetics (SMC2017), Banff, Canada, October
359 5-8, 2017.
- 360 9. Goldberg, D. E. *Genetic Algorithm in Search, Optimization, and Machine Learning*, Addison-Wesley, 1989.
- 361 10. Tan, T.-H.; Huang, Y.-F.; Liu, F.-T. Multi-user detection in DS-CDMA systems using a genetic algorithm
362 with redundancy saving strategy. *International Journal of Innovative Computing, Information and Control*
363 *(IJICIC)*, **2010**, *6*, 3347-3364.
- 364 11. Hasan, M.; Hossain, E. Distributed resource allocation for relay-aided device-to-device communication: a
365 message passing approach. *IEEE Trans. Wireless Commun.* **2014**, *13*, 6326-6341.
- 366 12. Chen, S.-H.; Chen, M.-C. Operators of the Two-Part Encoding Genetic Algorithm in Solving the Multiple
367 Traveling Salesmen Problem, In Proceeding of International Conference on Technologies and Applications
368 of Artificial Intelligence, pp. 331-336, Nov. 2011.
- 369 13. Tang, K.S.; Man, K. F.; Kwong, S.; He, Q. Genetic algorithms and their applications. *IEEE Signal Processing*
370 *Magazine*, **1996**, 22-37.